

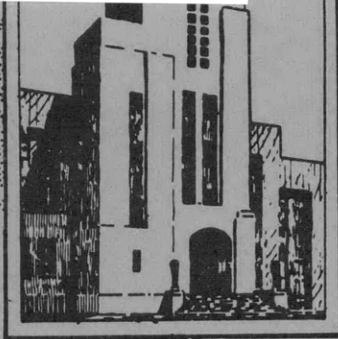
V393
R46

#1

MIT LIBRARIES



3 9080 02754 3625



DEPARTMENT OF THE NAVY
DAVID TAYLOR MODEL BASIN

HYDROMECHANICS

○

AERODYNAMICS

○

STRUCTURAL
MECHANICS

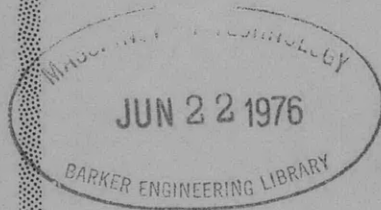
○

APPLIED
MATHEMATICS

PLASTIC PREBUCKLING STRESSES FOR RING-STIFFENED
CYLINDRICAL SHELLS UNDER EXTERNAL PRESSURE

by

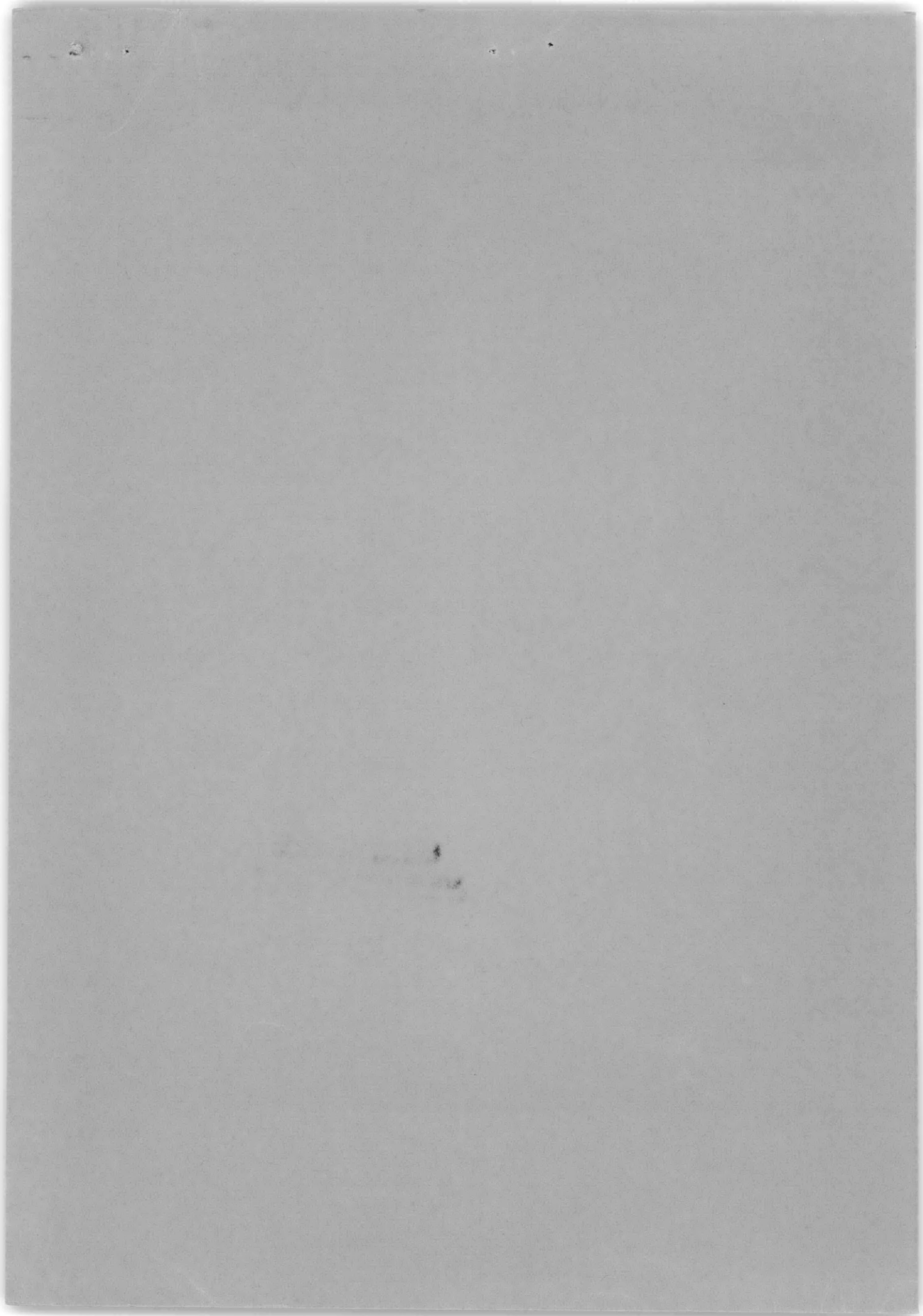
Myron E. Lurchick, Ph.D.



STRUCTURAL MECHANICS LABORATORY
RESEARCH AND DEVELOPMENT REPORT

January 1961

Report 1448



DEPARTMENT OF THE NAVY
DAVID TAYLOR MODEL BASIN
WASHINGTON 7. D.C.

IN REPLY REFER TO
9110/Subs
5605
(705:MCC:lkg)
Ser 7-37
2 February 1961

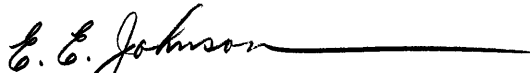
From: Commanding Officer and Director, David Taylor Model Basin
To: Chief, Bureau of Ships (Code 335) (in duplicate)

Subj: Plastic stresses in stiffened shell; forwarding of
report on

Encl: (1) DATMOBAS Report 1448 entitled "Plastic Prebuckling
Stresses for Ring-Stiffened Cylindrical Shells
under External Pressure" 3 copies

1. Recent developments in the design of closed stiffened cylinders loaded by external hydrostatic pressure have focused attention on the use of strain-hardening materials, such as aluminum, titanium, and steel with yield strengths above 125,000 psi. Hence, the David Taylor Model Basin has been investigating the buckling of the shell in the plastic range under Project S-F013 03 02. In enclosure (1) the plastic stresses and strains in a ring-stiffened cylindrical shell subjected to external hydrostatic pressure are determined from the deformation theory of plasticity. Strain hardening of the material is taken into account.

2. Strains determined by this theory agree well with experimental strains in the circumferential direction but are less than the experimental strains in the longitudinal direction.



E.E. JOHNSON
By direction

Copy to:

BUSHIPS (106) with 1 copy of encl (1)
(420) with 1 copy of encl (1)
(421) with 1 copy of encl (1)
(423) with 1 copy of encl (1)
(440) with 1 copy of encl (1)
(442) with 2 copies of encl (1)
(443) with 1 copy of encl (1)



9110/Subs
5605
(705:MCC:lkg)
Ser 7-37
2 February 1961

Copy to:

BUSHIPS {525} with 1 copy of encl (1)
{633} with 1 copy of encl (1)
CHONR {439} with 2 copies of encl (1)
{466} with 1 copy of encl (1)
CNO (Op 7020) with 1 copy of encl (1)
CDR, USNOL, with 1 copy of encl (1)
DIR, USNRL, Attn: TID (Code 2027) with 1 copy of encl (1)
NAVSHIPYD PTSMH, with 2 copies of encl (1)
NAVSHIPYD MARE, with 2 copies of encl (1)
NAVSHIPYD NORVA, Attn: UERD (280) with 1 copy of encl (1)
SUPSHIP, Groton, with 1 copy of encl (1)
Electric Boat Div, General Dynamics Corp, with 1 copy of
encl (1)
SUPSHIP, Newport News, with 1 copy of encl (1)
Newport News Shipbldg and Dry Dock Co, with 1 copy of
encl (1)
SUPSHIP, Pascagoula, with 1 copy of encl (1)
Ingalls Shipbldg Corp, with 1 copy of encl (1)
DIR, DEF (R and E) Attn: Tech Library, with 1 copy of
encl (1)
CO, USNROTC & NAVADMINU, MIT, with 1 copy of encl (1) ←
O in C, PGSCOL, Webb, with 1 copy of encl (1)
Prof. D.C. Drucker, Brown, with 1 copy of encl (1)
Prof. B. Budiansky, Harvard, with 1 copy of encl (1)
Prof. P.G. Hodge, Jr., Illinois Inst of Tech, with 1 copy
of encl (1)
Prof. N.J. Hoff, Stanford, with 1 copy of encl (1)
Dr. E. Wenk, Jr., Legislative Ref Service, Library of Congress,
with 1 copy of encl (1)
Dr. R.C. DeHart, Southwest Research, with 1 copy of encl (1)



ERRATA

for

David Taylor Model Basin Report 1448, January 1961

1. Four equations appearing on pages 4 and 5 are in error. These equations should read as follows:

$$D_p \frac{d^4 w}{dx^4} = P - \frac{\mu N_x}{R} - \frac{E_s h w}{R^2} - N_x \frac{d^2 w}{dx^2} \quad [14]$$

$$\frac{d^4 w}{dx^4} + 4 \alpha_p^4 \beta_p^2 \frac{d^2 w}{dx^2} + 4 \alpha_p^4 \left[w - \frac{PR^2}{E_s h} \left(1 - \frac{\mu}{2} \right) \right] = 0 \quad [17]$$

$$Z = \frac{PR^2}{E_s h} \left(1 - \frac{\mu}{2} \right) - w \quad [18]$$

$$\frac{d^4 Z}{dx^4} + 4 \alpha_p^4 \beta_p^2 \frac{d^2 Z}{dx^2} + 4 \alpha_p^4 Z = 0 \quad [19]$$

2. The shear forces shown in Figure 3 should be designated as minus, i.e.

$$- D_p \frac{d^3 w}{dx^3} \Big|_{x=0}$$



ERRATA SHEET

for

David Taylor Model Basin Report 1448 Dated January 1961

Page 3 Equation [8] reads $\epsilon_x = \epsilon_{mx} - z \frac{d^2 w}{dx^2}$

should read $\epsilon_x = \epsilon_{mx} + z \frac{d^2 w}{dx^2}$

Equation [10] reads $\sigma_x = \frac{E_s}{1 - \mu^2} \left[\epsilon_{mx} + \mu \frac{w}{R} - z \frac{d^2 w}{dx^2} \right]$

should read $\sigma_x = \frac{E_s}{1 - \mu^2} \left[\epsilon_{mx} + \mu \frac{w}{R} + z \frac{d^2 w}{dx^2} \right]$

Equation [11] reads $\sigma_\phi = \frac{E_s}{1 - \mu^2} \left[\frac{w}{R} + \mu \epsilon_{mx} - \mu z \frac{d^2 w}{dx^2} \right]$

should read $\sigma_\phi = \frac{E_s}{1 - \mu^2} \left[\frac{w}{R} + \mu \epsilon_{mx} + \mu z \frac{d^2 w}{dx^2} \right]$

The first part of the document discusses the importance of maintaining accurate records of all transactions. It emphasizes that every entry should be supported by a valid receipt or invoice. This not only helps in tracking expenses but also ensures compliance with tax regulations.

In the second section, the author outlines the various methods used to collect and analyze data. This includes both primary and secondary research techniques. The primary research involves direct observation and interviews, while secondary research involves analyzing existing data sources.

The third section focuses on the statistical analysis of the collected data. It describes the use of various statistical tests to determine the significance of the findings. The results indicate a strong correlation between the variables being studied, which supports the hypothesis of the research.

Finally, the document concludes with a summary of the key findings and their implications. It suggests that the results have important implications for the field of study and provides recommendations for further research.

**PLASTIC PREBUCKLING STRESSES FOR RING-STIFFENED
CYLINDRICAL SHELLS UNDER EXTERNAL PRESSURE**

by

Myron E. Lurchick, Ph.D.

January 1961

**Report 1448
S-F013 03 02**

TABLE OF CONTENTS

	Page
ABSTRACT	1
INTRODUCTION	1
THEORETICAL DERIVATION OF PLASTIC DEFORMATIONS	1
PROCEDURE FOR DETERMINING PLASTIC STRAINS	8
COMPARISON OF THEORY WITH EXPERIMENT	8
DISCUSSION	16
RECOMMENDATIONS	17
ACKNOWLEDGMENTS	17
REFERENCES	17

LIST OF FIGURES

Figure 1 – Variation of Strain and Poisson’s Ratio with Stress	2
Figure 2 – Notation for Coordinates and Deflections	3
Figure 3 – Forces Acting at a Stiffening Ring	6
Figure 4 – Scantlings of Models	9
Figure 5 – Stress-Strain Curves of Model Materials	9
Figure 6 – Circumferential Strain Plotted against Pressure	10
Figure 7 – Longitudinal Strain Plotted against Pressure	12
Figure 8 – Comparison between Plastic and Elastic $P - \sigma_i$ Plots	14

NOTATION

A	Area of frame
b	Faying width of frame
D_p	Plastic flexural rigidity
E	Modulus of elasticity
E_s	Secant modulus
h	Shell thickness
L	Effective frame spacing (center-to-center spacing minus b)
L_f	Center-to-center frame spacing
M	Moment
N	Force per unit width of shell
P	Pressure
R	Mean radius of shell
w	Radial deflection
x	Longitudinal coordinate
z	Radial coordinate
ϵ	Strain
ϵ_i	Strain intensity
μ	Poisson's ratio
μ_e	Elastic value of Poisson's ratio
σ	Stress
σ_i	Stress intensity

SUBSCRIPTS

x	Refers to longitudinal direction
m_x	Refers to membrane value in longitudinal direction
x_0	Refers to value on outer surface in longitudinal direction
x_i	Refers to value on inner surface in longitudinal direction
ϕ	Refers to circumferential direction
m_ϕ	Refers to membrane value in circumferential direction

ABSTRACT

The deformation theory of plasticity is used to determine the plastic stresses and strains in a ring-stiffened cylindrical shell subjected to external hydrostatic pressure. Strain-hardening of materials is taken into account. The plastic solution reduces to the elastic solution of Salerno and Pulos when the plastic modulus and the plastic Poisson's ratio are set equal to their corresponding elastic values. Strains determined by this theory agree well with experimental strains in the circumferential direction but are less than experimental strains in the longitudinal direction.

INTRODUCTION

Recent developments in the design of closed stiffened cylinders loaded by external hydrostatic pressure have focused attention on the use of strain-hardening materials, such as aluminum, titanium, and steel with yield strengths above 125,000 psi. The buckling of the shell in the plastic range for such cylinders has been investigated at the David Taylor Model Basin. Analytical solutions for the buckling pressure in both the axisymmetric and asymmetric modes are presented in References 1 and 2,^{*} respectively. The solutions for the plastic buckling pressure depend, however, on a knowledge of the prebuckling stresses. In References 1 and 2 the elastic solution of Salerno and Pulos³ was used to determine the critical pressure at which the prebuckling state of equilibrium and the buckling equation were satisfied simultaneously, but it was recognized that a plastic solution for the prebuckling stresses was needed before a plastic buckling equation could be strictly applicable.

A solution for the plastic prebuckling deformations of a closed cylindrical shell made from a strain-hardening material stiffened by uniformly spaced, transverse rings and subjected to external hydrostatic pressure is presented in this report. Theoretically determined plastic strains are then compared with those determined experimentally.

THEORETICAL DERIVATION OF PLASTIC DEFORMATION

The theory to be presented is essentially an extension of the *elastic* Salerno and Pulos theory to account for a variable material modulus and a variable Poisson's ratio. This extension is accomplished by using the deformation theory of plasticity.

Consider the stress-strain curve of a strain-hardening material shown in Figure 1. The biaxial state of stress existing in a thin cylindrical shell is related to the one-dimensional state of stress shown in Figure 1 by expressions for stress and strain intensities. The

^{*}References are listed on page 17.

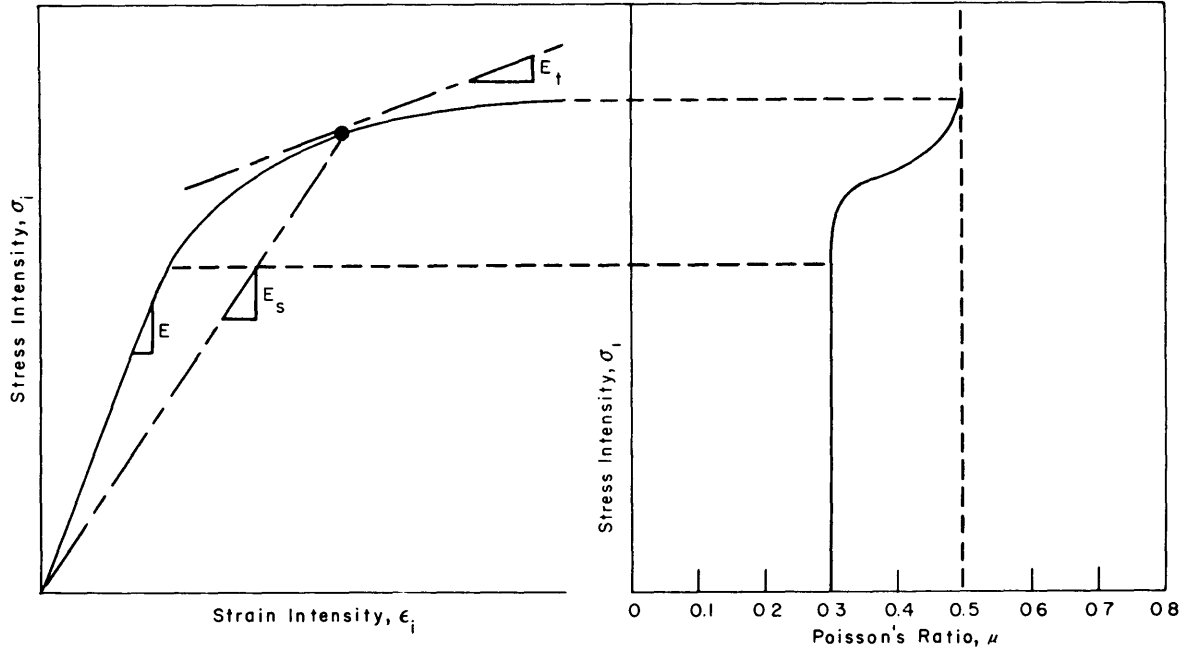


Figure 1 – Variation of Strain and Poisson's Ratio with Stress

expressions to be used are those presented in Reference 1 in which the deformation theory of plasticity has been generalized to include a variable Poisson's ratio rather than a fixed Poisson's ratio of $\frac{1}{2}$. Thus, considering only *principal* stresses and *principal* strains, one expresses these intensities as

$$\sigma_i = \sqrt{\sigma_x^2 + \sigma_\phi^2 - \sigma_x \sigma_\phi} \quad [1]$$

$$\epsilon_i = \frac{1}{1 - \mu^2} \sqrt{(1 - \mu + \mu^2)(\epsilon_x^2 + \epsilon_\phi^2) + (4\mu - \mu^2 - 1)\epsilon_x \epsilon_\phi} \quad [2]$$

The biaxial stress-strain relations consistent with Equations [1] and [2] are:

$$\sigma_x = \frac{E_s}{1 - \mu^2} (\epsilon_x + \mu \epsilon_\phi) \quad [3]$$

$$\sigma_\phi = \frac{E_s}{1 - \mu^2} (\epsilon_\phi + \mu \epsilon_x) \quad [4]$$

$$E_s = \frac{\sigma_i}{\epsilon_i} \quad [5]$$

Poisson's ratio is now a function of the state of stress. In Reference 1 the expression for Poisson's ratio is taken as that originally presented by Gerard and Wildhorn⁴ for an isotropic, plastically incompressible solid:

$$\mu = \frac{1}{2} - \left(\frac{1}{2} - \mu_e \right) \frac{E_s}{E} \quad [6]$$

where μ_e is the value of Poisson's ratio in the elastic region. The variation of μ with stress level is shown in Figure 1.

A portion of a stiffened cylinder is shown in Figure 2. The origin of the longitudinal coordinate x will be taken at a stiffening ring. Radial deflections w will be taken positive when inward. The pressure will be taken positive when externally applied.

For axisymmetric deformations the equation of equilibrium for a cylindrical shell is well-known as

$$-\frac{d^2 M_x}{dx^2} + \frac{N_\phi}{R} + N_x \frac{d^2 w}{dx^2} - P = 0 \quad [7]$$

Also, for axisymmetric deformations the total strains can be expressed as

$$\epsilon_x = \epsilon_{mx} + z \frac{d^2 w}{dx^2} \quad [8]$$

$$\epsilon_\phi = \frac{w}{R} \quad [9]$$

where ϵ_{mx} is the longitudinal membrane strain and z is the radial coordinate measured from the middle surface of the shell. Substituting Equations [8] and [9] into Equations [3] and [4] gives

$$\sigma_x = \frac{E_s}{1 - \mu^2} \left[\epsilon_{mx} + \mu \frac{w}{R} + z \frac{d^2 w}{dx^2} \right] \quad [10]$$

$$\sigma_\phi = \frac{E_s}{1 - \mu^2} \left[\frac{w}{R} + \mu \epsilon_{mx} + \mu z \frac{d^2 w}{dx^2} \right] \quad [11]$$

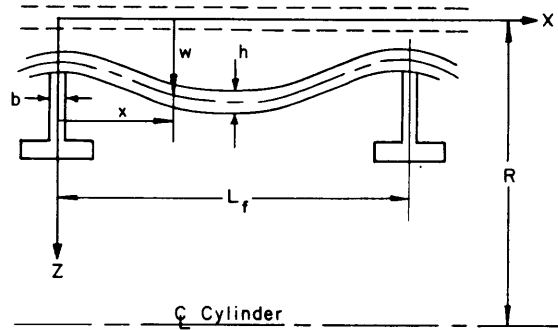


Figure 2 – Notation for Coordinates and Deflections

The longitudinal moment M_x and the circumferential force N_ϕ can be obtained by integration of stresses, thus:

$$M_x = \int_{-h/2}^{+h/2} \sigma_x z dz \quad [12]$$

$$N_\phi = \int_{-h/2}^{+h/2} \sigma_\phi dz \quad [13]$$

When Equations [10] and [11] are substituted into Equations [12] and [13] and the integrations are performed, the expressions for M_x and N_ϕ are identical to those obtained for the elastic case except that the secant modulus E_s replaces Young's modulus E . Accordingly, if the final expressions for M_x and N_ϕ are substituted into Equation [7], an equilibrium expression in terms of x will be obtained identical to the well-known elastic equation except that E_s replaces E , and μ replaces μ_e , thus,

$$D_P \frac{d^4 w}{dx^4} = P \frac{\mu N_x}{R} - \frac{E_s h w}{R^2} + N_x \frac{d^2 w}{dx^2} \quad [14]$$

where

$$D_P = \frac{E_s h^3}{12(1 - \mu^2)} \quad [15]$$

The longitudinal force N_x is simply

$$N_x = \frac{PR}{2} \quad [16]$$

Substituting Equations [15] and [16] into Equation [14] and rearranging terms, one obtains:

$$\frac{d^4 w}{dx^4} + 4\alpha_P^4 \beta_P^2 \frac{d^2 w}{dx^2} + 4\alpha_P^2 \left[w - \frac{PR^2}{E_s h} \left(1 - \frac{\mu}{2}\right) \right] = 0 \quad [17]$$

where

$$\alpha_P^4 = \frac{3(1 - \mu^2)}{R^2 h^2}$$

$$\beta_P^2 = \frac{PR^3}{2E_s h}$$

If a change is made in variable in Equation [17] as follows

$$Z = \frac{PR^2}{E_s h} \left(1 - \frac{\mu}{2}\right) - w \quad [18]$$

a simplified expression is obtained

$$\frac{d^4 Z}{dx^4} + 4\alpha_p^4 \beta_p^2 Z'' + 4\alpha_p^4 Z = 0 \quad [19]$$

where $Z'' = \frac{d^2 Z}{dx^2}$

To solve the final equilibrium expression, Equation [19], an assumption has to be made with regard to the secant modulus E_s . In reality, the secant modulus varies with the coordinates x and z since E_s is a function of the state of stress which varies with the deflection and curvature of the shell between stiffeners. The value of E_s will be determined for the shell on the basis of the membrane stresses at midbay and will be applied to the entire shell, i.e., E_s is a constant independent of coordinates x and z .

Although Salerno and Pulos have presented a solution to Equation [19], the solution to be shown is an equivalent one published previously in Reference 5, which is considered more convenient to use. For the boundary conditions

$$\begin{aligned} x = 0, L & \quad w = w_0 \\ x = 0, L & \quad \frac{dw}{dx} = 0 \end{aligned}$$

where w_0 is the deflection at a stiffener, the solution of Equation [19] is

$$Z = \frac{f(x)}{G} Z_0 \quad [20]$$

where

$$Z_0 = \frac{PR^2}{E_s h} \left(1 - \frac{\mu}{2}\right) - w_0 \quad [21]$$

$$\begin{aligned} f(x) = & K_2 \sinh K_1 x \cos K_2 (L - x) + K_1 \cosh K_1 x \sin K_2 (L - x) \\ & + K_1 \sin K_2 x \cosh K_1 (L - x) + K_2 \cos K_2 x \sinh K_1 (L - x) \end{aligned}$$

[22]

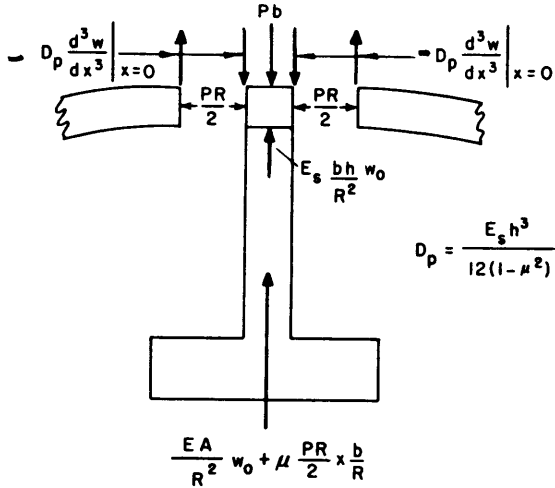


Figure 3 – Forces Acting at a Stiffening Ring

more, the stiffener is essentially stressed uniaxially, and, thus, longitudinal strains do not contribute to the stress in a stiffener. As a result, the stresses in a stiffener can remain elastic even though those in the shell are plastic. Accordingly, the modulus for a stiffener will be taken equal to Young's modulus E . The faying width will be considered to be a portion of the shell and to have a modulus E_s .

With these assumptions of moduli, the summation of forces at a frame is

$$2 D_p \frac{d^3 w}{dx^3} \Big|_{x=0} + \frac{EA}{R^2} w_0 + E_s \frac{bh}{R^2} w_0 - Pb + \mu \frac{Pb}{2} = 0 \quad [26]$$

In terms of the variable Z , Equation [26] becomes

$$\frac{d^3 Z}{dx^3} \Big|_{x=0} + 2\alpha_p^4 \left[\left(\frac{A}{h} \right) \frac{E}{E_s} + b \right] Z_0 - 4\alpha_p^4 \beta_p^2 \frac{A}{Rh} \cdot \frac{E}{E_s} \left(1 - \frac{\mu}{2} \right) = 0 \quad [27]$$

Substituting Equation [20] and its third derivative evaluated at $x = 0$ into Equation [27] and solving for Z_0 , one obtains:

$$Z_0 = 2\alpha_p^2 \beta_p^2 \frac{G}{H} \cdot \frac{A}{Rh} \cdot \frac{E}{E_s} \cdot \left(1 - \frac{\mu}{2} \right) \quad [28]$$

$$G = K_2 \sinh K_1 L + K_1 \sin K_2 L \quad [23]$$

$$K_1 = \alpha_p (1 - \alpha_p^2 \beta_p^2)^{1/2} \quad [24]$$

$$K_2 = \alpha_p (1 + \alpha_p^2 \beta_p^2)^{1/2} \quad [25]$$

The value of Z_0 can be obtained by considering the equilibrium of radial forces at the stiffening ring. The forces acting on a stiffener are shown in Figure 3. The circumferential stresses in a stiffening ring are always lower than those in the shell since the deflections are lowest at a stiffener. Furthermore,

where

$$H = \alpha_p^2 \left(\frac{AE}{hE_s} + b \right) G + 2K_1 K_2 (\cosh K_1 L - \cos K_2 L) \quad [29]$$

When Equations [18] and [28] are substituted into Equation [20], the expression for the deflection of the stiffened cylinder results:

$$w = \frac{\beta_p^2}{R} (2 - \mu) \left[1 - \frac{\alpha_p^2}{H} \frac{AE}{hE_s} f(x) \right] \quad [30]$$

It can be readily shown that the second derivative of Equation [30] is

$$\frac{d^2 w}{dx^2} = \frac{-2\alpha_p^4 \beta_p^4}{RH} (2 - \mu) \frac{AE}{hE_s} g(x) \quad [31]$$

where

$$\begin{aligned} g(x) = & K_1 \cosh K_1 x \sin K_2 (L - x) \\ & - K_2 \sinh K_1 x \cos K_2 (L - x) \\ & - K_2 \cos K_2 x \sinh K_1 (L - x) \\ & + K_1 \sin K_2 x \cosh K_1 (L - x) \end{aligned} \quad [32]$$

The strains can then be expressed in terms of w and $\frac{d^2 w}{dx^2}$ as

$$\epsilon_\phi = \frac{w}{R} \quad [33]$$

$$\epsilon_{x0} = \frac{(1 - \mu^2)}{E_s} \cdot \frac{PR}{2h} - \mu \frac{w}{R} - \frac{h}{2} \frac{d^2 w}{dx^2} \quad [34]$$

$$\epsilon_{xi} = \frac{(1 - \mu^2)}{E_s} \cdot \frac{PR}{2h} - \mu \frac{w}{R} + \frac{h}{2} \frac{d^2 w}{dx^2} \quad [35]$$

where the subscripts 0 and i refer to the outer and inner surfaces of the shell, respectively. The membrane stresses can be easily shown to be

$$\sigma_{mx} = \frac{PR}{2h} \quad [36]$$

$$\sigma_{m\phi} = E_s \epsilon_\phi + \mu \frac{PR}{2h} \quad [37]$$

The expressions for the membrane stresses are given as they will be used later in computing the stress intensity σ_i . Surface stresses can be obtained by using the strains determined by Equations [33], [34], and [35] together with Equations [3] and [4].

PROCEDURE FOR DETERMINING PLASTIC STRAINS

The plastic strains are determined by an iteration procedure. The secant modulus must be known, but E_s depends on the state of strain which is initially unknown.

Experience has shown that a good approach to the computations is to use the elastic solution for σ_i at midbay and at the middle plane for a specific pressure P . The stress-strain curve of the material is then entered to obtain ϵ_i . The secant modulus is obtained from Equation [5], and Poisson's ratio can subsequently be determined from Equation [6]. For given P and the values of E_s and μ , ϵ_ϕ is determined from Equation [33]. After membrane stresses are computed from Equations [36] and [37], the stress intensity is computed from Equation [1]. This value of σ_i usually will not differ widely from the value assumed. The procedure is repeated using this computed value of σ_i . Convergence between the assumed and the computed values of σ_i to three significant figures usually occurs rapidly, i.e., within three computational cycles.

When adequate agreement between the assumed and computed σ_i 's is obtained, $\frac{d^2w}{dx^2}$ can be determined from Equation [31] and, subsequently, the longitudinal surface strains can be determined from Equations [34] and [35].

COMPARISON OF THEORY WITH EXPERIMENT

Strains computed by the theory are compared with experimental strains from tests of four cylinders. The geometries of the cylinders are given in Figure 4. The stiffened cylinders, termed models, were made from thick forged tubes. The tubes were machined to form stiffening rings of T-section integrally attached to a thin shell. Models 1 and 2 were made of SAE-4340 steel and Models 3 and 4 of 7075-T6 aluminum. Stress-strain curves of the materials are shown in Figure 5. The elastic value of Poisson's ratio, μ_e , was taken as 0.3 for all models.

Pressure-strain plots for the models are presented in Figures 6 and 7. Figure 6 indicates good agreement between theory and experiment for the circumferential strains at both midbay and at a stiffening ring. On the other hand, Figure 7 indicates that, in the longitudinal direction, the theoretical plastic strains are usually smaller than the experimental strains at both midbay and at a stiffening ring. The discrepancy between theory and experiment increases with a rise in pressure. The theoretical plots of pressure versus longitudinal strain, however, do exhibit the pronounced nonlinearity indicated by the experimental data.

Geometric Parameter	Model			
	1	2	3	4
Shell Thickness Mean Diameter $= \frac{h}{D}$	0.00629	0.0100	0.0139	0.0177
Frame Spacing Mean Diameter $= \frac{L_f}{D}$	0.101	0.224	0.126	0.263
Faying Width Frame Spacing $= \frac{b}{L_f}$	0.0250	0.0168	0.0601	0.0385
Area of Frame Area of Shell $= \frac{4}{hL_f}$	0.579	0.270	0.646	0.321

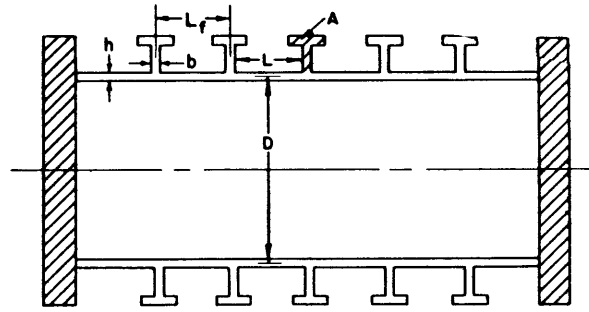


Figure 4 – Scantlings of Models

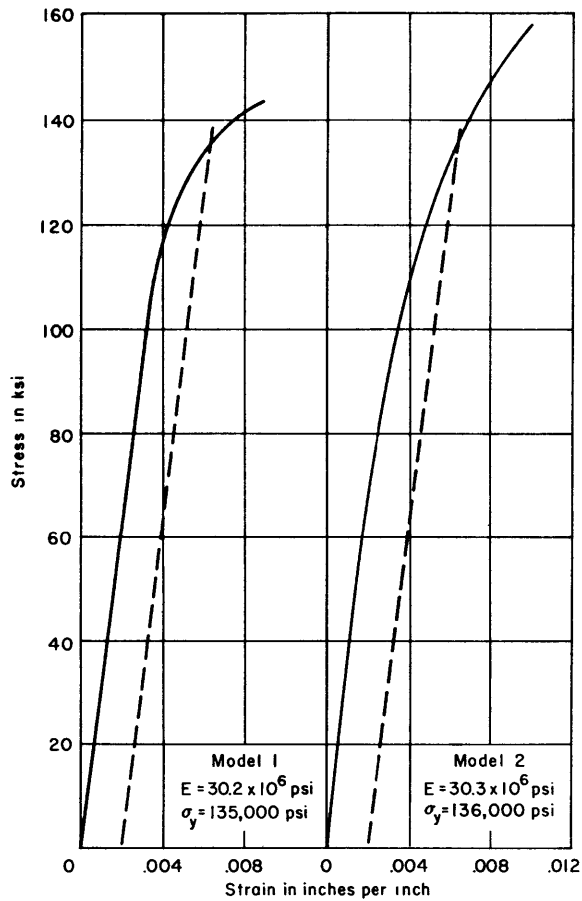


Figure 5a – Steel

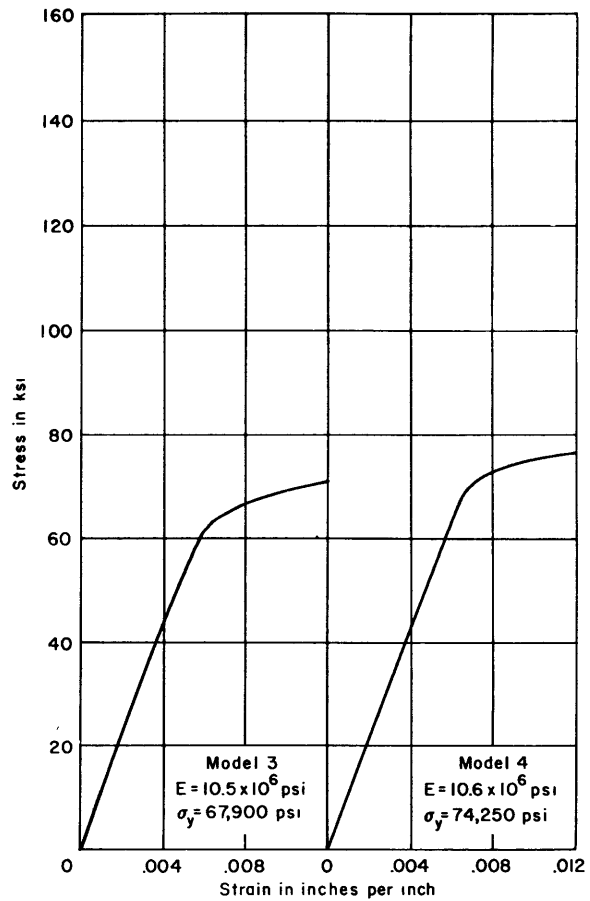


Figure 5b – Aluminum

Figure 5 – Stress-Strain Curves of Model Materials

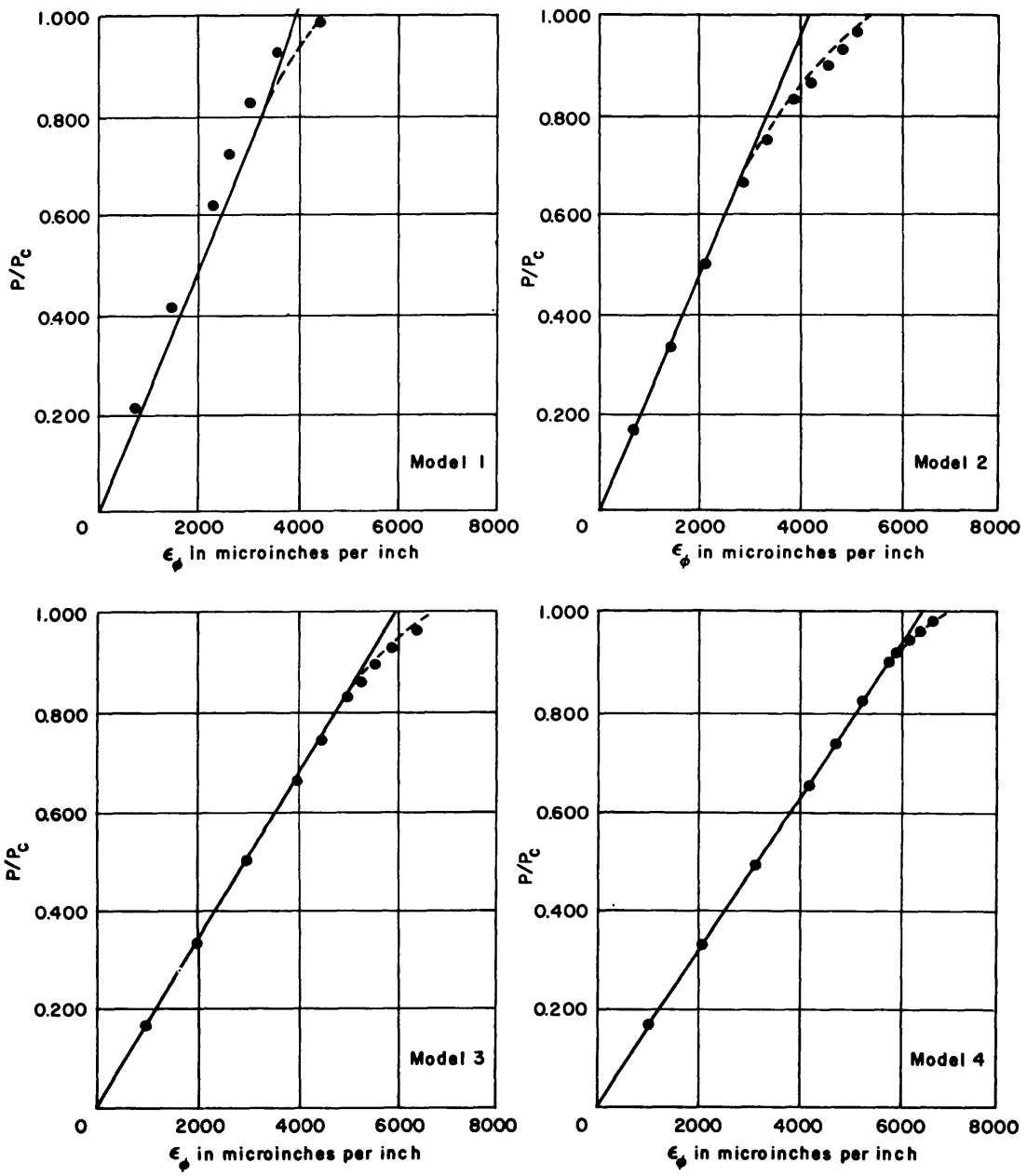


Figure 6a - At Midbay

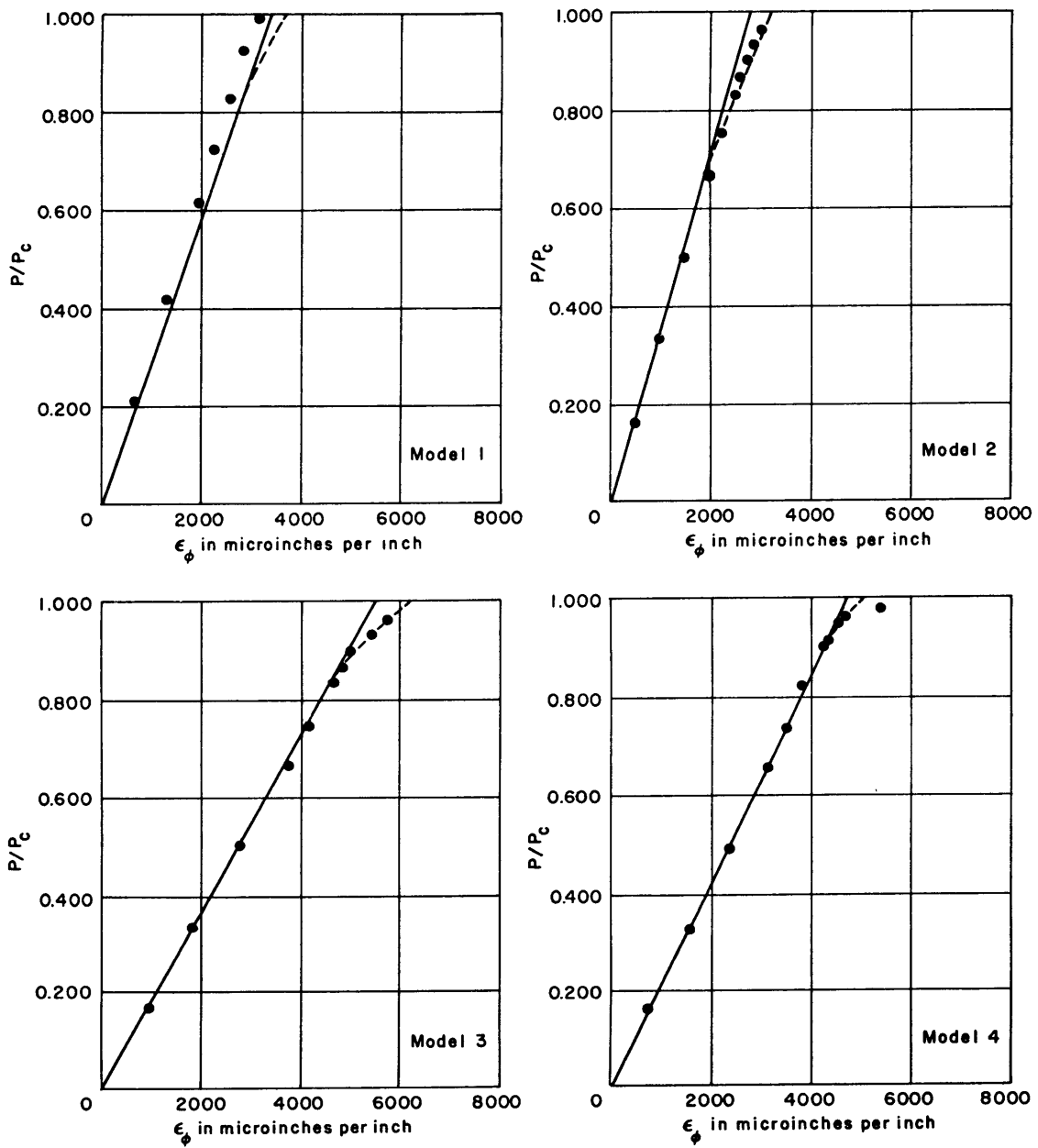


Figure 6b – At a Stiffening Ring

Figure 6 – Circumferential Strain Plotted against Pressure

Circumferential strain	ϵ_ϕ	Experimental strains	●
Applied pressure	P	Elastic theory	—
Collapse pressure	P_c	Plastic theory	- - -

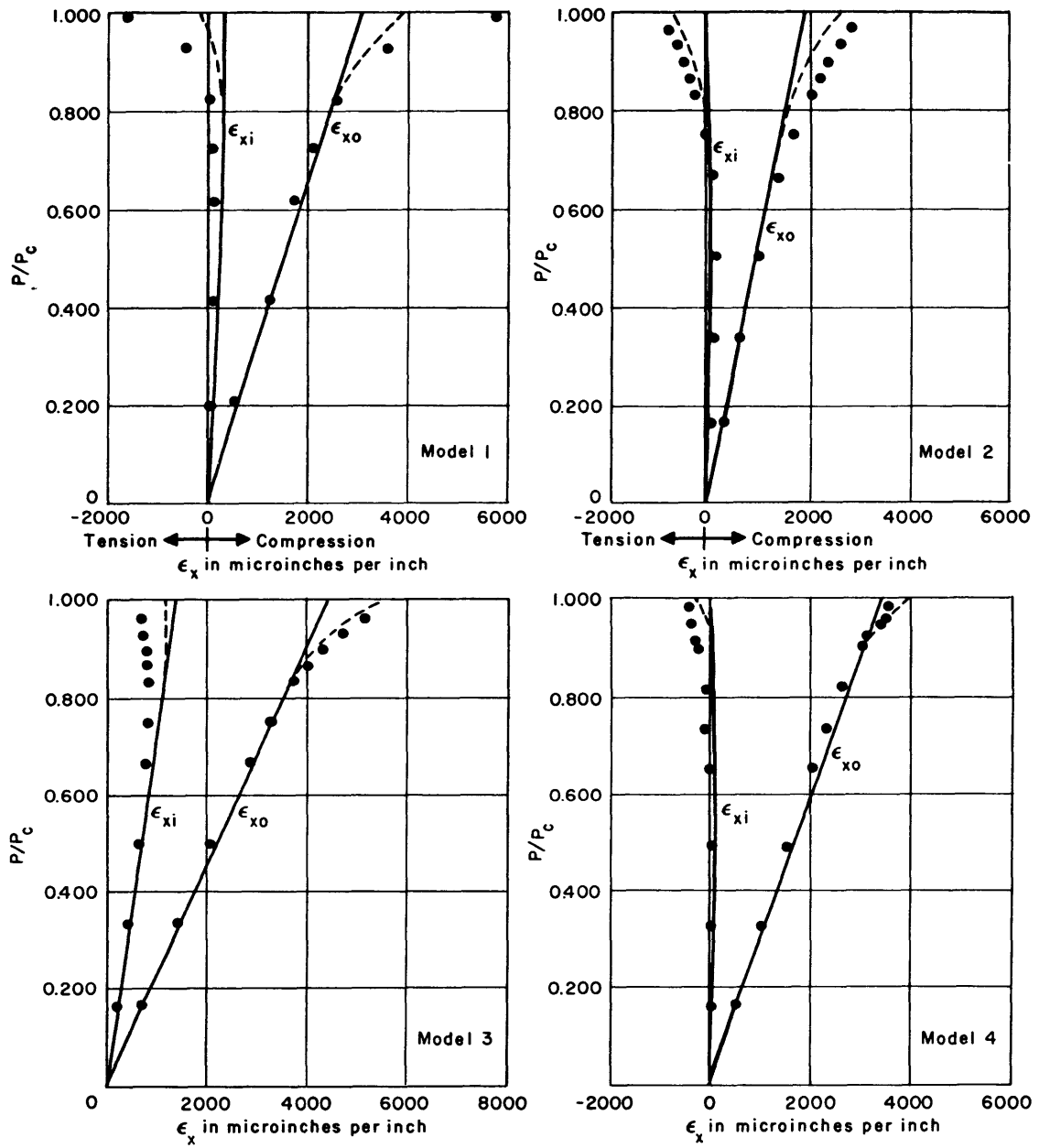


Figure 7a – At Midbay

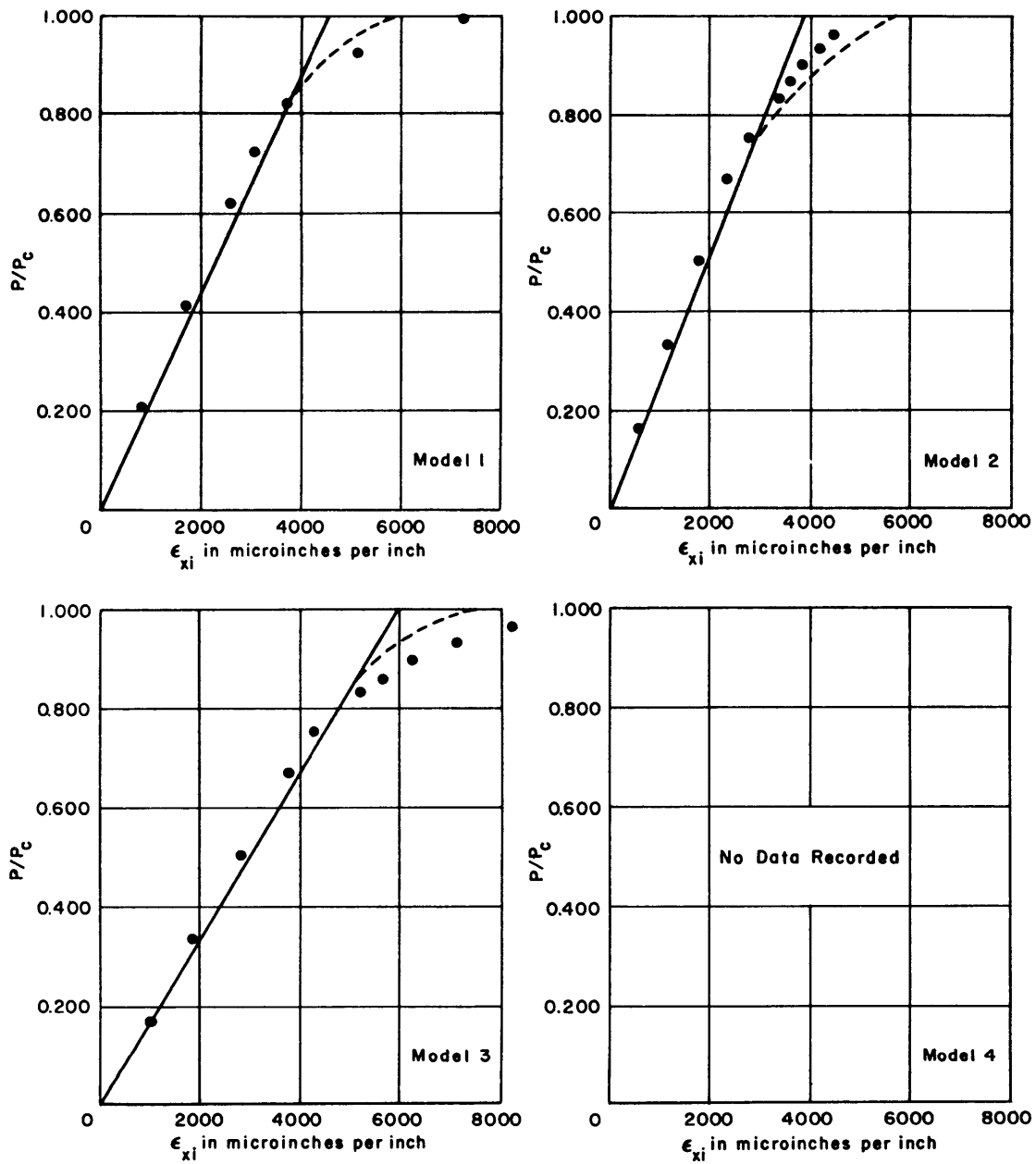


Figure 7b – At a Stiffening Ring

Longitudinal strain	ϵ_x	Collapse pressure	P_c
Outside longitudinal strain	ϵ_{x0}	Experimental strains	•
Inside longitudinal strain	ϵ_{xi}	Elastic theory	—————
Applied pressure	P	Plastic theory	- - - - -

Figure 7 – Longitudinal Strain Plotted against Pressure

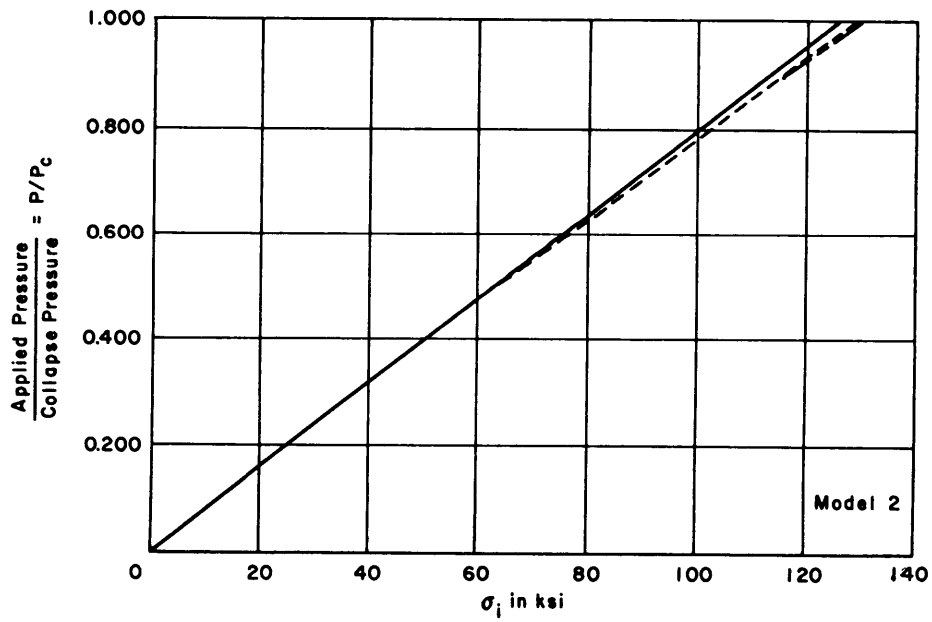
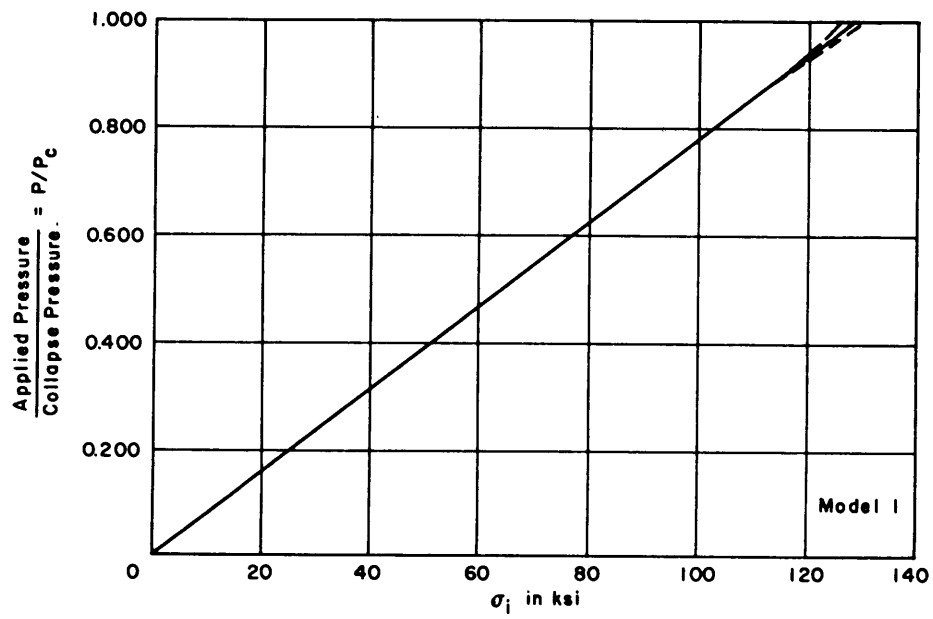


Figure 8a – Steel Models

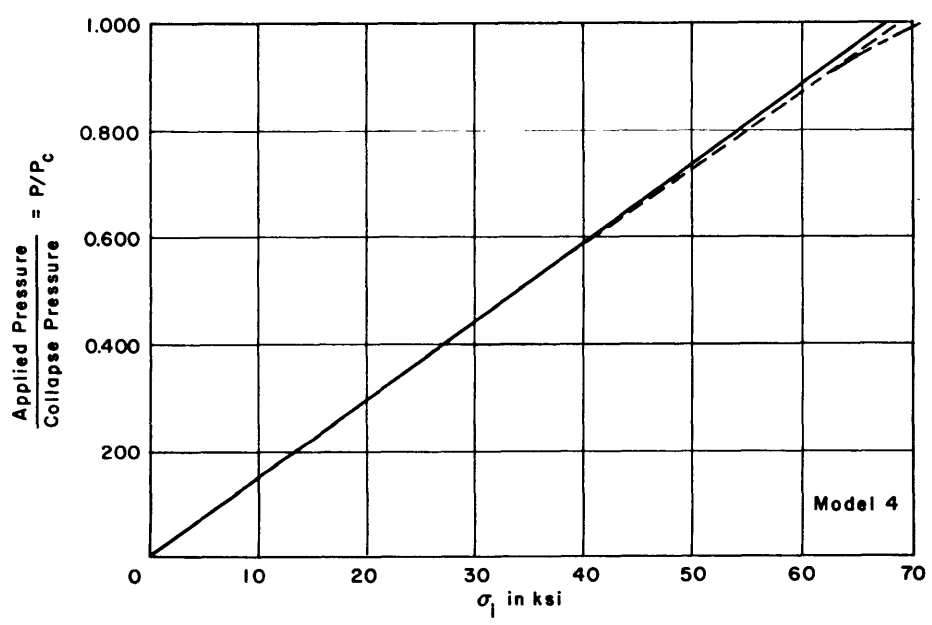
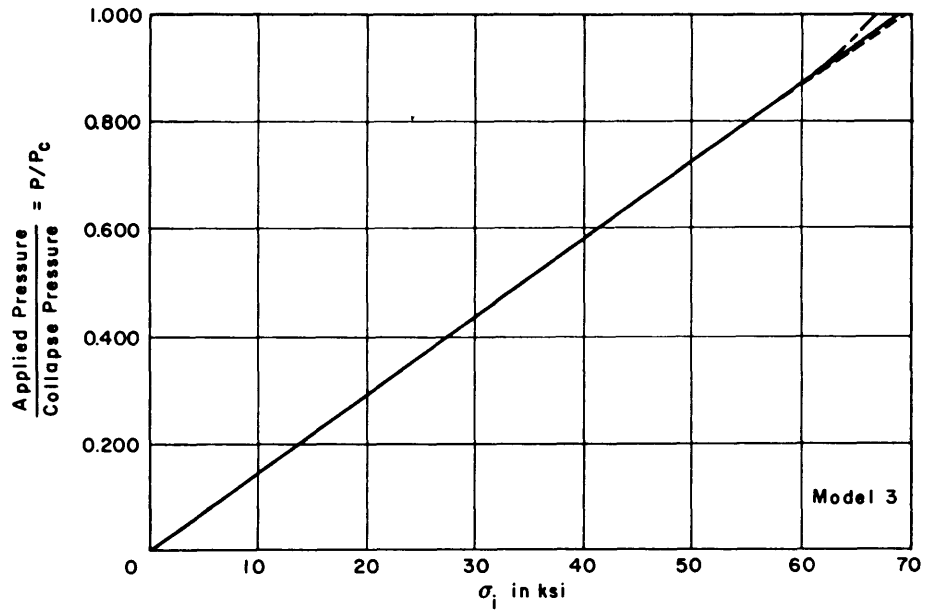


Figure 8b – Aluminum Models

Proportional loading —————

Elastic theory - - - - -

Plastic theory - . - . - .

Figure 8 – Comparison between Plastic and Elastic $P - \sigma_i$ Plots

DISCUSSION

One of the prime motivations behind this theoretical analysis is the more accurate determination of $P - \sigma_i$ plots. These plots are used to determine the plastic buckling pressures. Figure 8 presents $P - \sigma_i$ plots for the four models tested. It can be seen that the $P - \sigma_i$ plots determined by the plastic theory do not differ very much from those determined by the elastic theory. Apparently, the use of the elastic solution of Salerno and Pulos to determine the plastic buckling pressure is good approximation for the four models reported. However, the use of an elastic solution for σ_i could conceivably result in large errors in the determination of collapse pressure for other ranges in cylinder geometry.

Figure 8 also indicates that both the elastic and plastic $P - \sigma_i$ plots do not depart appreciably from the linear $P - \sigma_i$ plot. The linear plot characterizes proportional loading in which the beam-column effect due to the end loads is neglected. Budiansky⁶ has shown the extent to which deviations from proportional loading may be allowed when deformation theory is used and still not violate the general requirements for the physical soundness of a plasticity theory. Since the deviations from proportional loading are small and well within the range delimited by Budiansky, the use of the deformation theory of plasticity instead of the incremental theory is justified.

The merits of this plastic analysis are:

1. The plastic theory reduces to the accepted elastic theory of Salerno and Pulos when $E_s = E$ and $\mu = \mu_e$. As a result, no discontinuities occur in the pressure-strain relationships.
2. The stress-strain curve is not replaced by an approximation, e.g., elastic, perfectly plastic or rigid plastic materials. The actual stress-strain curve for the material is used.
3. The pronounced nonlinearity in the pressure-strain relationships is indicated by the theory.

The limitations in the analysis are:

1. The secant modulus is taken independent of the axial or radial coordinates x and z . The variation of E_s with x is usually not too large, but the variation with z can be appreciable.
2. Small-deflection theory is used; therefore, the analysis is confined to deflections less than one-half the shell thickness.
3. The stiffening ring is assumed to be elastic always; hence, the analysis is not applicable when yielding penetrates into the stiffener.

RECOMMENDATIONS

1. The theory should be extended to include variations of E_s through the shell thickness. In other words, the analysis should account for nonlinear variations of the bending stresses through the thickness.
2. The theory should be extended to include yield penetration into the stiffening rings.

ACKNOWLEDGMENTS

The author is indebted to Dr. S.R. Bodner of Brown University for his suggestions in the formulation of the analysis. Mr. R.D. Short of the David Taylor Model Basin checked the equations in the analysis.

REFERENCES

1. Lunchick, M.E., "Plastic Axisymmetric Buckling of Cylindrical Shells of Strain-Hardening Materials Subjected to External Hydrostatic Pressure," David Taylor Model Basin Report 1393 (in preparation).
2. Reynolds, T.E., "Inelastic Lobar Buckling of Cylindrical Shells under External Hydrostatic Pressure," David Taylor Model Basin Report 1392 (Aug 1960).
3. Salerno, V.L. and Pulos, J.G., "Stress Distribution in a Circular Cylindrical Shell under Hydrostatic Pressure," Polytechnic Institute of Brooklyn Aeronautical Laboratory Report No. 171-A (1951).
4. Gerard, G. and Wildhorn, S., "A Study of Poisson's Ratio in the Yield Region," National Advisory Committee for Aeronautics Technical Note 2561 (Jan 1952).
5. Lunchick, M.E. and Short, R.D., "Behavior of Cylinders with Initial Shell Deflection," Journal of Applied Mechanics, Transactions ASME, Vol. 24, No. 4 (Dec 1957). Also David Taylor Model Basin Report 1150 (Jul 1957).
6. Budiansky, B., "A Reassessment of Deformation Theories of Plasticity," Journal of Applied Mechanics, Vol. 26, Series E, No. 2 (Jun 1959).

INITIAL DISTRIBUTION

Copies

- 13 CHBUSHIPS
 - 3 Tech Info Br (Code 335)
 - 1 Tech Asst (Code 106)
 - 1 Prelim Des Br (Code 420)
 - 1 Prelim Des Sec (Code 421)
 - 1 Ship Protec (Code 423)
 - 1 Hull Des Br (Code 440)
 - 2 Sci & Res Sec (Code 442)
 - 1 Struc Sec (Code 443)
 - 1 Sub Br (Code 525)
 - 1 Hull Arrgt, Struc, & Preserv (Code 633)
- 3 CHONR
 - 2 Struc Mech Br (Code 439)
 - 1 Undersea Programs (Code 466)
- 1 CNO (Op 702C)
- 1 CDR, USNOL
- 1 DIR, USNRL (Code 2027)
- 2 NAVSHIPYD PTSMH
- 2 NAVSHIPYD MARE
- 1 NAVSHIPYD NORVA, Attn: UERD (Code 280)
- 1 SUPSHIP, Groton
- 1 Electric Boat Div, General Dyn Corp, Groton
- 1 SUPSHIP, Newport News
- 1 NNSB & DD Co
- 1 SUPSHIP, Pascagoula
- 1 Ingalls Shipbuilding Corp
- 1 Dir, Def R & E, Attn: Tech Library
- 1 CO, USNROTC & NAVADMINU, MIT
- 1 O in C, PGSCOL, Webb
- 1 Prof. D.C. Drucker, Brown
- 1 Prof. B. Budiansky, Harvard
- 1 Prof. P.G. Hodge, Jr., Illinois Inst of Tech
- 1 Prof. N.J. Hoff, Stanford

Copies

- 1 Dr. E. Wenk, Jr., Legislative Ref Service,
Library of Congress
- 1 Dr. R.C. DeHart, Southwest Research

MIT LIBRARIES DUPL

3 9080 02754 3625

DEC 23 1978